Manuscript

Different functional roles and expression of miR-126-3p and miR-126-5p in breast cancer cell lines and tissues

Charles Johannessen[1]*, Yury Kiselev[2], Mona Irene Pedersen[3], Stig Manfred Dalen[4], Lill-Tove Rasmussen Busund[1, 4], Eiliv Lund[5], Karina Standahl Olsen[5], Line Moi[1, 4]

[1] Department of Medical Biology, UiT - The Arctic University of Norway, Tromsø, Norway

[2] Department of Life Sciences and Health, OsloMet – Oslo Metropolitan University, Oslo, Norway

[3] Department of Clinical Medicine, UiT - The Arctic University of Norway, Tromsø, Norway

[4] Department of Clinical Pathology, University Hospital of North Norway, Tromsø, Norway

[5] Department of Community Medicine, UiT - The Arctic University of Norway, Tromsø, Norway

* E-mail: charles.johannessen@uit.no

Abstract

Background

MiRNAs are regulators of gene expression and are involved in carcinogenesis through regulation of oncogenes, tumor suppressors and cellular oncogenic properties such as invasion and metastasis. MiR-126 has tumor suppressor function in various cancers, and seems to regulate the metastatic process in BC both *in vitro* and *in vivo*.

Methods

Functions of miR-126-3p and the passenger strand miR-126-5p were explored in the ER+ breast cancer cell line MCF7, HER2+ SK-BR-3 cells and triple negative MDA-MB-231 cells using the proliferation platform xCelligence and invasion assay CytoSelect Cell Invasion. MiRNA expression in malignant and benign breast tissue were analyzed by microarray and RT-PCR, and cell specific in-tumor fibroblasts and epithelium using ISH and tissue microarrays.

Results

MiR-126-3p transfection led to decreased proliferation and invasion in all cell lines, whereas miR-126-5p had the opposite effect in MDA-MB-231 cells where miR-126-5p was the dominant strand determined by RT-PCR analysis. Both miR-126 strands were downregulated in cancer compared to benign tissue, and in lymph node positive breast cancers compared to tumors without nodal involvement. MiR-126-5p ISH stromal staining was significantly higher in high grade tumors and in stroma and tumor cells of luminal B, HER2 positive and triple negative tumors compared to luminal A.

Conclusions

MiR-126-3p has tumor suppressor functions in breast cancer cell lines. MiR-126-5p, however, promotes proliferation and invasion in triple negative cancer cells and demonstrates higher expression in tumors of high grade and aggressive molecular subtypes. Different functions and expression of the miR-126 strands in breast cancer subtypes add to the complexity of miRNAs' regulatory network in malignant disease.

Introduction

Breast cancer (BC) in women accounts for 30% of all new cancer cases, and is the most common cancer diagnosed worldwide in the female population [1, 2]. BC is a highly heterogeneous malignancy, contributing to the challenges of determining the most effective treatment regimens [3, 4]. There are different approaches to subgrouping of BC, where tumor grade, TNM-stage (tumor, node, metastasis), molecular subtype and/or receptor status are the principal categories [5-9]. Despite extensive efforts to improve prognosis in BC patients, it remains the second largest cause of cancer related deaths in women [1, 2, 4]. More than 90% of BC mortality is due to local recurrence and distant metastases [10, 11]. Cells from the primary tumor are known to metastasize and disseminate in the bone marrow at a presymptomatic stage in the tumorigenesis, and may persevere in a dormant state for years, even decades, before becoming clinically evident, contributing to the challenges in accurate diagnosis, treatment and follow-up [4, 12]. Improving the prognostic and predictive biomarkers for early detection of primary and metastatic disease, alongside with the identification and stratification of the most aggressive tumors with focus on targeted treatments, still needs to be a priority in BC research.

MicroRNAs (miRNAs) constitute a conserved class of endogenous small non-coding RNAs first discovered in *Caenorhabditis elegans* [13]. They function as post-transcriptional gene expression regulators and, depending on the degree of base complementarity to the 3’ untranslated region (3’-UTR) of target mRNAs, they suppress gene expression by either complete mRNA degradation, mRNA destabilization, or mRNA silencing [14-16]. According to the miRBase database of published miRNA sequences and annotations, there are currently described more than 2500 unique mature miRNAs [17].

In BC, various miRNAs have been studied, where some contribute to the upregulation of oncogenes, while others activate tumor suppressor genes [18, 19]. Moreover, studies have shown that miRNA expression profiles vary between different subcategories of BC [20, 21]. Some of the best described miRNAs differentially expressed in BC, are the miR-200 family and the miR-21 [22, 23]. The miR-200 family consists of five individual miRNAs, and they are suppressed during epithelial to mesenchymal transition (EMT), a central step in metastasis and cancer progression [24, 25]. MiR-21 is highly expressed in BC, and has been shown to inhibit several tumor suppressors in BC. High expression of miR-21 is associated with overall tumor progression and poor prognosis [23, 26]. It is of great interest to investigate and characterize individual miRNAs, their expression and functional roles in BC and their subtypes.

MiR-126 was initially described as a regulator of megakaryocytopoiesis and leukemia [27], but has since been designated a tumor suppressor role in various cancers [28-31]. Reduced expression of miR-126 has been linked to invasion and metastasis, especially through the regulation of ADAM9 [32-34], and miR-126 has been described as predicting response to chemotherapy and bevacizumab treatment [35]. Noteworthy, miR-126 has been shown to be a negative regulator of metastatic progression, mainly through downregulation of key functions such as cell proliferation, migration, and survival of BC cells [36].

Through a series of *in vitro* experiments, we sought to study the functional effects of both miR-126-3p, and its passenger strand miR-126-5p, in BC cell lines reflecting different subtypes of breast cancer: Estrogen receptor positive (ER+), human epithelial growth factor receptor positive (HER2+), and triple negative (TN) BCs. Using an unselected cohort of BC patients participating in the Norwegian Woman and Cancer Study (NOWAC) [37], we further wanted to evaluate the

tissue- and cell specific expression of miR-126-3p and miR-126-5p using *in situ* hybridization methods.

Methods

Functional studies

To investigate the functional properties of miR-126-3p and miR-126-5p in tumorigenesis, we performed a series of *in vitro* experiments. A miR-126-3p and a miR-126-5p mimic were introduced into different BC cell lines. The miRNAs were introduced alone or in combination, alongside a miRNA negative control, to study cell proliferation and cell invasion.

Cell cultures

The functional properties of miR-126-3p and miR-126-5p were evaluated in three different BC cell lines: the ER+ cell line MCF7 (ATCC ® HTB-22™), the HER2+ cell line SK-BR-3 (ATCC® HTB-30™), and the triple negative (TN) cell line MDA-MB-231. SK-BR-3 and MDA-MB-231 were cultured in RPMI-1640 media (cat.# R8758, Sigma-Aldrich, St. Louis, USA) supplemented with 10% fetal bovine serum (cat.# S0415, Biochrom, Berlin, Germany). MCF7 cells were cultured in DMEM (cat.# D5796, Sigma-Aldrich, St. Louis, USA) with the same supplements as the other two cell lines. All cell lines were incubated at 37°C in a humidified atmosphere with 5% CO_2. Additionally, total RNA from the non-cancerous breast cell line MCF-10A was used in qPCR experiments. This was as a kind gift from the RNA and molecular pathology (RAMP) research group, UiT - The Arctic University of Norway, Tromsø, Norway.

Cell transfection

BC cell lines were transiently transfected with 100 nM hsa-miR-126-3p Pre-miR™ miRNA Precursor (cat.# PM12841, Thermo Fisher Scientific, USA) and/or 100 nM hsa-miR-126-5p Pre-

miR™ miRNA Precursor (cat.# PM10401, Thermo Fisher Scientific, USA), alongside the Cy3™ Dye-Labeled Pre-miR Negative Control #1 (cat.# AM17120, Thermo Fisher Scientific, USA). The transfection was performed using 8 µl/mL of the Lipofectamine® RNAiMAX transfection reagent (cat.# 13778075, Thermo Fisher Scientific, USA). Transfected Cy3™ Dye-Labeled Pre-miR Negative Control emits fluorescent light when exposed to UV-light to allow detection of transfected cells, and the transfection efficiency was determined using a fluorescence microscope. The transfection efficiency was typically as high as 80% - 95%.

Total RNA isolation

Total RNA was isolated from cells using the miRNeasy Mini Kit (cat.# 217004, Qiagen, Hilden, Germany) according to the manufacturer's protocol. Briefly, cells were lysed using 700 µl QiAzol Lysis Reagent before homogenization and incubation for 5 minutes at room temperature. Next, 140 µl chloroform were added, and the samples were shaken before incubation at room temperature for 3 minutes. Samples were then centrifuged for 15 minutes at 12000 g at 4°C, and the upper aqueous phase was transferred and mixed thoroughly with 100% ethanol. Finally, samples were transferred into the RNeasy® Mini column and washed in several steps before elution with 50 µl ddH_2O. Isolated total RNA samples were stored at -70°C.

cDNA synthesis

Synthesis of first strand cDNA was performed using the miScript II RT Kit (cat.# 218160, Qiagen, Hilden, Germany) according to the manufacturer's protocol. In short, 100 ng of total RNA was mixed with 4 µl 5x miScript HiSpec Buffer, 2 µl 10x Nucleics Mix, 2 µl miScript Reverse Transcriptase Mix, and RNase-free water to a total volume of 20 µl. Next, samples were incubated for 60 minutes at 37°C, and subsequently incubated for 5 minutes at 95°C to inactivate enzymes. Finally, samples were diluted with 200 µl RNase-free water and stored at -20°C.

RT-PCR

Endogenous levels of miR-126-3p and miR-126-5p in the BC cell lines were quantified relative to the reference snRNA RNU6 using the miScript SYBR® Green PCR Kit (cat.# 218073, Qiagen, Hilden, Germany) and real-time PCR. The primers used in this study were miScript Primer Assays Hs_miR-126_1 miScript Primer Assay (cat.# MS00003430, Qiagen, Hilden, Germany), Hs_miR-126*_1 miScript Primer Assay (cat.# MS00006636, Qiagen, Hilden, Germany), and Hs_RNU6-2_11 miScript Primer Assay (cat.# MS00033740, Qiagen, Hilden, Germany), and all primers were used according to the manufacturer's protocol. Briefly, a total volume of 25 µl/well in a 96-well plate included 1 µl cDNA mixed with 12.5 µl 2x QuantiTect SYBR Green PCR Master Mix, 2.5 µl 10x miScript Universal Primer, 2.5 µl 10x miScript Primer Assay, and 6.5 µl RNase-free Water. The plate was sealed and centrifuged for 1 minute at 1000 g before it was placed in a 7300 Real-Time PCR System (Thermo Fisher Scientific, Waltham, Massachusetts, USA). Each sample was analyzed in quadruplicates, and three independent experiments were performed.

Proliferation assay

The real-time cell analyzer system xCelligence, RTCA DP (cat#05469759001, ACEA Biosciences, San Diego, USA) fitted with the E-plate 16 (cat#05469830001, ACEA Biosciences, San Diego, USA) was used to study the proliferation of the BC cell lines. Cells were trypsinized until detached, resuspended in complete growth media and counted before analysis on the xCelligence platform. Approximately 8000 cells per well were estimated to be optimal through initial titration experiments. In line with the manufacturer's protocol, cells were seeded in quadruplicates into an E-plate after baseline measurements, and the E-plate incubated for 30 minutes at room temperature before being positioned in the RTCA DP instrument. The

instrument was located in an incubator preserving the same conditions as used for routine cultivation of cell lines. The cellular growth rate is denoted as 'Cell Index' and recorded by the instrument every 30 minutes, where the index is an arbitrary unit reflecting the cell-sensor impedance. The RTCA software version 1.2.1 was used to calculate growth curves. Three independent experiments were performed as a minimum for each cell line.

Invasion assay

The invasiveness of the BC cell lines was tested using the CytoSelect™ 96-well Cell Invasion Assay, Basement membrane (cat.# CBA-112, Cell Biolabs, San Diego, USA) according to the manufacturer's protocol. In short, a modified Boyden chamber was used, and 50000 pretransfected and serum starved cells were seeded in the upper chamber precoated with a basement membrane (a protein matrix isolated from Engelbreth-Holm-Swarm tumor cells). The cells were allowed to invade for 24 h towards the bottom chamber containing media +10% FBS. Cancer cells that were able to invade and pass through the porous membrane to the bottom side of the membrane were lysed and stained before fluorescence was measured at 480/520 nm using the CLARIOstar® microplate reader (BMG LABTECH, Ortenberg, Germany). All experiments were performed in quadruplicates. Three independent experiments were performed as a minimum for each cell line.

Classification of human breast cancer samples

The patient samples included in the study were retrieved from the archives at the Department of Pathology at the University Hospital of North Norway in Tromsø and the Nordland Hospital in Bodø. The BC cases were NOWAC participants diagnosed with breast cancer in the years 2004 – 2010. FFPE tissue cores from breast reduction surgery specimens were included in the study as benign tissue controls. Histological grading and immunohistochemical (IHC) analyses of ER,

progesterone receptor (PR) and HER2 were done as part of routine diagnostics, but validated by a breast pathologist (L.M.). Cut-off values for ER positivity was ≥ 1%, for PR ≥ 10 % and for HER2 score 3+. Silver in situ hybridization (SISH) was done when HER2 IHC was inconclusive (score 2+). The proliferation marker Ki67 was evaluated in at least 500 tumor cells in the most proliferative areas of the tumor on slides from the primary surgery and reported as percentage of positive tumor cells. Molecular subtyping of tumors was based on the surrogate markers ER, PR, HER2 and Ki67 according to recommendations by the St Gallen International Expert Consensus and previous publications [38, 39] as presented in table 1:

Table 1: Molecular subtyping of tumors based on surrogate markers.

	ER/PR	HER2	Ki67
Luminal A	ER+ and/or PR+	−	≤30%
Luminal B	ER+ and/or PR+	Any	>30% if HER2−
HER2 positive	−	+	Any
Basal like	−	−	Any

MiRNA microarray and validation by PCR

Tissue cores from formalin-fixed paraffin-embedded (FFPE) tissue blocks where collected. Total RNA was extracted from the tissue cores using the RecoverAll Total Nucleic Acid Isolation kit (Life Technologies, Grand Island, NY, USA) according to the manufacturer's instructions, and RNA quality and quantity assessed using the NanoDrop 1000 spectrophotometer (Thermo Fisher Scientific, Wilmington, DE). Exiqon (Vedbaek, Denmark) performed the microarray hybridization and analyses as a paid service. In summary, 250 ng total RNA from samples and reference were labeled with Hy3TM and Hy5TM, using the miRCURY LNATM microRNA Hi-Power Labeling Kit (Exiqon). An aliquot of all RNA species included in the study was used as

the Hy5TM-labeled reference RNA. Samples and reference RNA were mixed before hybridization on a Tecan HS4800 hybridization station (Tecan, Austria) to the 7th generation miRCURY LNA microRNA array containing probes for miRNAs in human, mouse and rat as annotated in miRBASE version 19.0. Slides were scanned on the Agilent G2565BA Microarray Scanner System (Agilent technologies Inc., USA) before image analysis using the ImaGene 9.0 software (BioDiscovery Inc., USA). The detection threshold was set as 1.2 times the 25th percentile of the overall signal intensity of individual slides.

Forty tumor samples and 20 of the benign breast tissue controls were included in PCR validation, also performed by Exiqon. RNA was extracted from FFPE tissue cores according to the manufacturer's instruction using the Qiagen miRNeasy FFPE kit (Qiagen, Hilden, Germany), and 10 ng RNA was reverse transcribed using the miRCURY LNA Universal RT microRNA PCR, Polyadenylation and cDNA synthesis kit (Exiqon). 100 x diluted cDNA went into PCR-reactions using ExiLENT SYBR Green master mix in 384 well plates on a Light Cycler 480 Real-Time PCR System (Roche). Suitable reference miRNAs were evaluated by Exiqon using the Normfinder software. Based on stable expression across the data set, miR-664a-3p was used for normalization. The expression values were calculated using the quantification cycle (Cq) from PCR analyses and the formula: average Cq (all samples) – assay Cq (sample).

Tissue microarray

Full histological slides of tumor tissue from resection specimens were evaluated by two pathologists (L.M. and L.T.B) and representative areas of tumor tissue carefully selected and marked. The tissue microarray (TMA) was constructed using a tissue-arraying instrument (Beecher Instruments, Silver Spring, MD) as previously published [40]. In short, a 0.6 mm-diameter stylet was used to collect a total of four replicate tissue cores from each donor block and

transferred to the recipient block. 4 µm sections were cut with a Microm microtome HM355S (Microm, Walldorf, Germany) and used for hematoxylin and eosin staining and later *in situ* hybridization.

In situ hybridization

The miRNA in situ hybridization (ISH) was performed in Ventana Discovery Ultra instrument (Ventana Medical Systems Inc, Arizona, USA). Reagents were supplied by Roche (Bacel, Switzerland). Labelled locked nucleic acid (LNA) modified probes and controls were delivered by Exiqon (Vedbaek, Denmark). For this study, the hsa-miR-126-3p (619866-360), hsa-miR-126-5p (612156-360), U6 snRNA positive control probe and Scramble-miR negative control probe were used. Exiqon analyzed the LNATM oligonucleotides by CE or HPLC, and confirmed the identity of compound by MS.

First, 4 µm breast TMA sections were cut with a Micron microtome (HM355S) and placed on SuperFrost Plus glass slides. Second, sections were incubated at 60°C overnight to melt the paraffin and increase attachment to the slides. During the process of sectioning and staining, cautions were taken to prevent RNase contamination of reagents and degradation of the RNA samples.

As positive and negative tissue controls, sections from a TMA multi-organ tissue block were used. It included benign and malign tissue from 12 different human organs.

Hybridization conditions were optimized for temperature and concentration for each LNA probe. For breast TMA FFPE, a hybridization temperature of 51°C gave specific staining for both miR-126-3p and miR-126-5p. The best staining intensity for miR-126-3p was achieved at a concentration of 2 nM, while for the miR-126-5p the optimal concentration was 10 nM.

Sensitivity level of the ISH protocol was consolidated by clean and strong staining with 0.5 nM U6 snRNA. Concentrations between 0.1-2.0 nM were required for optimal sensitivity. Scramble miR negative control probe gave negative staining at standard conditions. For deparaffinization, pretreatments and chromogen staining, the well-established standard ISH protocols in the Discovery Ultra instrument were used. This methodology is described in more detail in our previous publication on miRNAs [41].

Scoring of ISH staining intensity

For semiquantitative evaluation of ISH staining intensities for miR-126-3p and -5p, TMA tissue slides were used. For each sample, a minimum of two tissue cores of tumor tissue and tumor-associated stromal tissue were evaluated using a microscope at 200x magnification. By morphologic criteria, tumor cells and stromal fibroblasts were scored for staining intensity with the dominant staining intensity scored as: 0 = negative, 1 = weak, 2 = moderate, 3 = strong. From the observed ISH staining pattern, both tumor cells and stromal fibroblasts stained diffusely and homogenously and hence staining density was not scored since it did not give any additional information. All cores were independently scored by two pathologists (L.M. and S.M.D.) who were blinded to each other's score and histopathological parameters. In case of disagreement (score discrepancy > 1), the slides were re-examined and a consensus was reached by the observers. Mean score for each case was calculated from both cores and both examiners.

Statistics

The descriptive statistics, the non-parametric tests, and the correlation analysis were performed using IMB SPSS Statistics, version 25. Standard error for the qPCR quantification and the invasion study was calculated using four technical replicates from a representative experiment. Statistics in the proliferation experiments were calculated using one-way ANOVA with p-values

corrected for multiple testing by controlling the false discovery rate implementing the method of Benjamini & Hochberg.

Results

Relative expression of miR-126-3p and miR-126-5p in breast cancer cell lines

To evaluate the endogenous expression of miR-126-3p and miR-126-5p, miRNA levels in BC cell lines were quantified relative to the levels in the non-cancerous breast cell line MCF-10A. RT-qPCR revealed downregulated levels of both miR-126-3p and miR-126-5p in all three BC cell lines (Fig. 1A). Noteworthy, the highest relative levels of the lead strand, miR-126-3p, compared to the passenger strand, miR-126-5p, were observed in the non-cancerous breast cell line MCF-10A, whilst the lowest relative levels were observed in the TN BC cell line MDA-MB-231 (Fig. 2). Interestingly, in contrast to the other cell lines, miR-126-5p appears to be more abundant than miR-126-3p in the TN BC cell line (Fig. 2).

Functional studies of miR-126-3p and miR-126-5p *in vitro*

The potential functional roles of miR-126-3p and miR-126-5p in the three BC cell lines were explored by *in vitro* experiments. Effects on proliferation and invasion were evaluated after transfecting the BC cell lines with either miR-126-3p mimic, miR-126-5p mimic or both in combination and in equal concentrations.

Transfection of miR-126-3p inhibits proliferation and invasion *in vitro*

All three BC cell lines demonstrated a significant drop in proliferation when transfected with miR-126-3p (Fig. 3). Depending on the cell line, the shift in proliferation occurred 12-48 hours after transfection.

Further, the invasive potential of all three cell lines were significantly reduced when transfected with miR-126-3p (Fig. 4). The degree of inhibition seemed to be uniform across cell lines, independent of receptor status.

Transfection of miR-126-5p increases proliferation and promotes invasion in the TN BC cell line MDA-MB-231

The proliferation rate, as denoted by cell index, of the TN cell line MDA-MB-231 was significantly increased when transfected with miR-126-5p mimic. The effect was highly significant, reproducible, and was observed almost immediately after transfection (Fig. 3C). In contrast, the proliferation rates of the ER+ and HER2+ BC cell lines were reduced compared to negative control, although not to the same extent as for cells transfected with miR-126-3p (Fig. 3A-B).

In the invasion experiment, where cells were allowed to invade and migrate through a basement membrane matrix, the TN cell line MDA-MB-231 displayed an increase in invasive ratio after

transfection with miR-126-5p (Fig. 4). In contrast, the invasion ratios of the ER+ and HER2+ cell lines were not significantly different in cells transfected with miR-126-5p compared to negative control (Fig. 4).

Cotransfection of miR-126-3p and miR-126-5p inhibits proliferation and invasion *in vitro*

Cotransfecting miR-126-3p and miR-126-5p in equal concentrations resulted in a tumor suppressor phenotype in all BC cell lines (Fig. 4). In the cell lines MCF-7 and SK-BR-3, where both miR-126-3p and miR-126-5p alone demonstrated inhibition of proliferation and invasion, the combination of the two demonstrated a similar effect, and the magnitude of this inhibition was comparable to that of miR-126-3p alone (Figs. 3A-B, 4). Transfecting miR-126-5p into the TN cell line resulted in an increase in both proliferation and invasion, but the cotransfection of both miRNAs in equal concentration resulted in inhibition of proliferation and invasion (Figs. 3C, 4). Again, the magnitude of this inhibition was equivalent to that of miR-126-3p transfection alone.

Expression of miR-126-3p and miR-126-5p in the BC patient cohort using microarray and PCR

A total of 108 NOWAC BC cases from the postgenome cohort and 44 benign tissue controls were included in the study. One case had to be excluded because of insufficient amount of tumor tissue and five cases and six controls were excluded due to poor RNA quality, leaving 102 BC cases and 38 benign tissue controls to be analyzed using miRNA microarray. An additional case and two of the controls were identified as outliers after microarray and excluded from further statistical analyses. 40 tumor samples and 20 of the controls were included in PCR validation.

Table 1 presents the expression levels of miR-126-3p and -5p in the BC tumors and benign tissue controls.

Microarray miRNA analysis revealed a significant downregulation of both miR-126-3p and miR-126-5p in BC tissue compared to benign breast tissue ($p<0.001$). This result was validated and confirmed by PCR analyses ($p<0.001$) (Fig. 1B and Table 2). Microarray- and PCR-based expression levels were significantly correlated for both miR-126-3p ($r=0.47$, $p<0.001$) and miR-126-5p ($r=0.46$, $p<0.001$). Noteworthy, we found lower expression of miR-126-3p and -5p in tumors with lymph node metastases compared to breast cancer cases without nodal involvement (Table 2 and Fig. 5). Further subgroup analyses did not demonstrate any significant differences in the expression of any of the miR-126 strands between tumors of different histological grade or molecular subtype.

Table 2: Histopathological variables and descriptive data for breast cancer cases and controls with miR-126-3p and miR-126-5p expression data.

		PCR		Array	
		miR-126-3p	**miR-126-5p**	**miR-126-3p**	**miR-126-5p**
Control	**Mean**	4,24	-0,86	9,28	7,16
	SD	0,79	0,8	1,13	0,52
	N (%)	20 (100)	20 (100)	38 (100)	38 (100)
All tumors	**Mean**	3,02	-2,01	7,38	6,13
	SD	0,33	0,32	0,49	0,19
	N (%)	40 (100)	40 (100)	102 (100)	102 (100)
	P*	**<0.001**	**<0.001**	**<0.001**	**<0.001**
Tumor grade 1	**Mean**	3,21	-1,81	7,44	6,17
	SD	1,1	1,03	0,42	0,20
	N (%)	7 (17.5)	7 (17.5)	31 (32)	31 (32)
Tumor grade 2	**Mean**	3,29	-1,75	7,30	6,10
	SD	0,8	0,72	0,49	0,18
	N (%)	17 (42.5)	17 (42.5)	41 (41)	41 (41)
Tumor grade 3	**Mean**	2,55	-2,46	7,43	6,10
	SD	1,15	1,14	0,53	0,17
	N (%)	16 (40)	16 (40)	26 (27)	26 (27)
	P*	0.269	0.356	0.536	0.328
Luminal A	**Mean**	3,13	-1,91	7,38	6,14
	SD	0,8	0,64	0,49	0,19
	N (%)	12 (30)	12 (30)	54 (54.5)	54 (54.5)
Luminal B	**Mean**	3,14	-1,84	7,41	6,13
	SD	1,41	1,37	0,37	0,16
	N (%)	11 (27.5)	11 (27.5)	20 (21.5)	20 (21.5)
HER2+	**Mean**	3,11	-1,99	7,56	6,18
	SD	0,88	0,78	0,54	0,16
	N (%)	7 (17.5)	7 (17.5)	9 (8)	9 (8)
Basal-like	**Mean**	2,52	-2,48	7,26	6,06
	SD	0,94	1,01	0,54	0,20
	N (%)	10 (25)	10 (25)	16 (16)	17 (16)
	P*	0.866	0.917	0.716	0.514
Lymph node pos	**Mean**	2,44	-2,63	7,22	6,06
	SD	0,76	0,65	0,45	0,16
	N (%)	11 (27)	11 (27)	31	31
Lymph node neg	**Mean**	3,18	-1,82	7,48	6,17
	SD	1,04	0,98	0,47	0,19
	N (%)	29 (73)	29 (73)	69	69
	P*	**0.049***	**0.010***	**0.021***	**0.025***

Stromal ISH expression of miR-126-5p increases with both histological grade and molecular subtype

The cellular and subcellular expression of miR-126-3p and miR-126-5p in BC tissue was evaluated by ISH in TMA slides, and staining intensity in tumor cells and fibroblasts scored as a semiquantitative measure of miRNA expression (Fig. 6). ISH staining for both strands of miR-126 was cytoplasmic and observed in malignant epithelial cells and cancer-associated stromal fibroblasts. Further, it was noted positive staining for miR-126-3p and -5p in endothelial cells and inflammatory cells within the tumor.

In TMA, 90 of the BC tumors had representative tissue cores with tumor and stromal cells represented, from which ISH staining intensity could be analyzed. Noteworthy, positive ISH staining for miR-126-3p and -5p was observed in all tumors. The mean score for miR-126-3p in tumor and stroma was 2.22 and 2.60, respectively, compared to 1.35 in tumor and 1.09 in stroma for miR-126-5p. Mean miR-126-5p staining intensity in tumor cells was significantly different in tumors grouped according to molecular subtype ($p=0.006$) where subgroup analyses revealed a significantly lower miR-126-5p expression in tumor cells of luminal A tumors compared to luminal B ($p=0.035$), HER2+ ($p=0.011$) and basal-like cancers ($p=0.012$) (Fig. 7A).

Interestingly, the main differences in expression of miR-126 between tumor groups were found when exploring the staining of miR-126-5p in the stromal compartment. The stromal expression of miR-126-5p was significantly different between tumors of different histological grade with lower expression in grade 1 tumors compared to grade 3 ($p=0.006$) (Fig. 7B), and in luminal A tumors compared to luminal B ($p=0.022$), HER2 positive ($p=0.002$) and the basal-like subgroup ($p<0.001$) (Fig. 6A). Both miR-126-3p and -5p staining in tumor cells and stroma was higher in ER- compared to ER+ tumors, whereas HER2+ tumors had higher miR-126-5p staining in tumor

cells and stroma compared to HER2- tumors. There were no significant differences in miR-126-3p and -5p mean staining intensity in tumor or stromal cells between tumors according to lymph node status, although the lowest levels were found in tumors with nodal metastases. ISH scores according to histopathological variables are presented in Table 3.

Table 3: In situ hybridization scores for miR-126-3p and miR-126-5p. Data presented as mean score in tumor cells and stroma of breast cancer tumors according to histopathological variables.

		miR-126-3p		miR-126-5p	
		Tumor	**Stroma**	**Tumor**	**Stroma**
Histological grade	**Grade 1**	2.14	2.59	1.19	0.80
	Grade 2	2.22	2.64	1.35	1.11
	Grade 3	2.31	2.57	1.52	1.38
	P	0.67	0.83	0.094	**0.023***
Molecular subtype	**Luminal A**	2.13	2.56	1.17	0.76
	Luminal B	2.21	2.60	1.52	1.21
	HER2+	2.39	2.50	1.72	1.78
	Basal-like	2.39	2.80	1.48	1.63
	P	0.35	0.11	**0.006***	**<0.001****
ER status	**Positive**	2.14	2.56	1.27	0.84
	Negative	2.42	2.71	1.56	1.67
	P	**0.042***	**0.017***	**0.008***	**<0.001****
HER2 status	**Positive**	2.22	2.58	1.62	1.53
	Negative	2.22	2.61	1.30	1.00
	P	0.97	0.98	**0.029***	**0.027***
Lymph node status	**Positive**	2.12	2.52	1.28	0.94
	Negative	2.27	2.64	1.39	1.16
	P	0.32	0.20	0.20	0.16

There was a positive correlation between the ISH staining intensity in tumor cells and stromal fibroblasts for both miR-126-3p and miR-126-5p (Table 4). Interestingly, the proliferative marker Ki67 displayed a positive correlation with the stromal expression of miR-126-5p which was borderline significant at the $p \leq 0.05$ level ($r=0.24$, $p=0.055$).

Table 4: Correlation of miR-126-3p and miR-126-5p from *in situ* hybridization staining.

			miR-126-3p		miR-126-5p		Ki67
	N=90		Tumor	Stroma	Tumor	Stroma	*N=63*
miR-126-3p	Tumor	r		0.47**	0.42**	0.29**	0.09
	Stroma	r			0.24*	0.39**	0.11
miR-126-5p	Tumor	r				0.70**	0.18
	Stroma	r					0.24(*)

Discussion

Herein, we describe the miR-126-3p and its passenger strand, miR-126-5p, in BC using both functional studies of BC cell lines and studies of the miRNAs' expression patterns in samples from BC patients.

Endogenous expression of miR-126-3p and miR-126-5p was found to be downregulated both in malignant tumors from women participating in the NOWAC study, and in the three different cell lines representing the BC subtypes ER+, HER2+, and TN tumors. This is in line with other studies where expression of miR-126 has been reported to be downregulated in malignant compared to benign breast tissue [42]. Promoter regulation of the host gene of miR-126, *EGFL7*, has been reported as a possible underlying mechanism [30, 43].

Expression of miR-126-3p is considered tumor suppressive [30, 44-46], and the functional experiments presented in this study support this perception, as all three studied BC cell lines

displayed inhibition of both proliferation and invasion when transfected with miR-126-3p. Interestingly, the passenger strand, miR-126-5p, appears to be a potent driver of tumorigenesis in the TN cell line MDA-MB-231, whilst having tumor suppressive effects in the ER+ MCF7 and the HER2+ SK-BR-3 cell line. Proliferation and invasion significantly increased in the TN cell line when transfected with miR-126-5p. The effect was profound, especially in the proliferation assays, and this was reproduced in a minimum of three independent experiments. Other studies of miR-126 in BC have reported the passenger strand miR-126-5p to be a tumor suppressor working in synergy with the lead strand, miR-126-3p [30, 47]. However, there are reports of miR-126-5p being associated with tumor promoting properties, such as drug resistance and poor prognosis in acute myeloid leukemia (AML) patients [48], promotion and protection of endothelial proliferation by inhibition of Dlk1 and SetD5 [49, 50], and induction of proliferation and angiogenesis in non-tumorigenic cells via the PI3K/AKT and MAPK/ERK pathways [51]. Interestingly, the epidermal growth factor-like protein Delta-like homolog 1 (Dlk1) is suppressed by miR-126-5p, but not miR-126-3p, in endothelial cells [49]. Dlk1 is an inhibitor of NOTCH-receptors, which, depending on cellular context, have oncogenic or tumor suppressor properties. Low levels of Dlk1 and thereby higher levels of NOTCH-signaling have been reported to increase cell proliferation and cell invasion of MDA-MB-231 cells [52], the TN BC cell line used in our study. Further, transfection of miR-126-5p in other cell types has been shown to inhibit the expression of the *klotho* gene, and increase the phosphorylation of Akt [53]. Klotho exerts inhibitory effects on the IGF-1 signaling pathway and has tumor suppressive effects in BC cells [54]. Downregulation of klotho and Dlk1 represents possible underlying mechanisms for the observed tumor promoting effects of miR-126-5p in the TN BC cell line in our study.

For the ER+ and the HER2+ cell lines, transfection with miR-126-5p led to a tumor suppressive response in the proliferation experiments, although the effect was less pronounced when compared to the experiments with the lead strand, miR-126-3p. Notably, when transfecting the ER+ and HER2+ BC cell lines using miR-126-5p, their invasion potential did not significantly differ to that of the control transfection.

The passenger strands of miRNAs are typically degraded after processing, and are consequently less abundant compared to their lead strand [15]. This is also evident for mature miR-126 in our study, where expression of miR-126-3p in the patient cohort and the BC cell lines MCF7 and SK-BR-3 is greater compared to expression of miR-126-5p. Interestingly, when comparing endogenous levels of miR-126-3p with endogenous levels of miR-126-5p in the non-cancerous cell line MCF-10A, the ER+ BC cell line MCF-7, the HER2+ BC cell line SK-BR-3, and the TN BC cell line MDA-MB-231, we found an incremental shift in the miR-126-3p/miR-126-5p expression pattern. The non-cancerous cell line MCF-10A appears to harbor the largest relative amount of miR-126-3p, followed by ER+ MCF-7 and HER2+ SK-BR-3, whilst the TN MDA-MB-231 has the opposite expression pattern, with miR-126-5p presenting as the more abundant strand. It is possible that mechanisms responsible for targeting the passenger strand miR-126-5p for degradation are either corrupted or in some way modified to allow miR-126-5p to accumulate. As a consequence, a larger part of the mature passenger strand, miR-126-5p, is eligible to interact with the RISC-complex to exhibit a more potent biological response in the TN BC cell line which represents the most aggressive BC subtype (Fig. 8).

Studies of miRNA biogenesis, expression and functions have reported that different miRNA strands can be selected in a tissue specific manner and during cancer progression [55, 56]. Further, high abundance of target mRNAs may block miRNA release from their targets and

protect miRNA strands from degradation by exoribonucleases [56]. Hence, regulation of miRNA strand selection and stability could add to the complexity of miRNA expression and function in different BC subtypes, as illustrated by the different functions of miR-126-3p and miR-126-5p in different BC cell lines in the present study.

In the clinical tumor samples, the expression of miR-126-3p and -5p, analyzed by microarray and PCR, was lower in lymph node positive breast cancers compared to tumors without nodal metastases. Interestingly, miR-126 has been shown to be a negative regulator of the metastatic process in BC in part by suppressing tumor growth *in vitro* using highly metastatic breast cancer cell lines [36]. In a murine model of breast cancer, miR-126 knockdown cells were shown to form metastases with high blood vessel density due to increased recruitment of endothelial cells to the metastatic cells [57]. The target genes demonstrated to mediate the suppressive effects of miR-126 on metastasis formation were *IGFBP2,* the receptor kinase *MERTK* and the phosphatidylinositol transfer protein *PITPNC1,* which in sum mediate a positive migratory and chemotactic signal to endothelial cells.

The expression of miR-126-3p and -5p was not significantly different between tumors of different histological grade or molecular subtype when analyzed using microarray and PCR technology. The homogenized tissue used for RNA extraction and later microarray and PCR contains RNA contributions not only from epithelial cells, but also from other cellular components in benign and malignant tissue such as fibroblast, endothelial cells, adipocytes and lymphocytes. However, in this study, ISH analysis of both miRNA strands was included, allowing us to explore the *in situ* expression of miR-126 in both tumor and stromal BC cells. Interestingly, stromal levels of miR-126-5p were significantly associated with both molecular subtype and histological grade, with the highest levels of miR-126-5p observed in the tumors

belonging to the BC subtypes with the worst prognosis. Although not statistically significant (p=0.055), the positive correlation between miR-126-5p and the proliferation marker Ki67 is noteworthy in this context. These findings are especially interesting when considering the *in vitro* experiments where the introduction of miR-126-5p produced a more aggressive phenotype in the TN BC cell line MDA-MB-231. The linkage between miR-126-5p expression and BC subtype and grade was highly significant in BC stroma, i.e. in fibroblasts within the tumor. Fibroblasts are involved in tumorigenesis and constitute the majority of stromal cells in breast tumors [58]. Several studies have described considerable crosstalk between tumor and stroma via exosomal transfer of miRNAs [59-61] where microvesicles containing miRNAs derived from cancer cells convert fibroblast into cancer associated fibroblasts (CAFs) with tumor-promoting properties. Further, exosomes from fibroblast can also affect cancer cell functions, e.g. miRNAs from CAFs have been shown to be directly involved in ER repression in breast cancer through secreted exosomes [62]. Hence, the increased stromal miR-126-5p expression and its association with more advanced breast cancers is an interesting finding, given the diversity of miR-126-5p effects in functional studies.

This study has increased our understanding and awareness of miRNAs duplexity in regulation and function. Through *in vitro* studies we have described the mature miR-126 as having both potent tumor suppressor and tumor driver functions with opposite effects of the two different miR-126 strands in TN BC. Functional studies on individual miRNAs are an important tool in detecting and understanding these two-faced properties which are recurrently emerging for several miRNAs.

References

1. Miller KD, Siegel RL, Lin CC, Mariotto AB, Kramer JL, Rowland JH, et al. Cancer treatment and survivorship statistics, 2016. CA Cancer J Clin. 2016;66(4):271-89. doi: 10.3322/caac.21349. PubMed PMID: 27253694.
2. Cancer Facts & Figures 2017. American Cancer Society. 2017.
3. Yadav BS, Sharma SC, Chanana P, Jhamb S. Systemic treatment strategies for triple-negative breast cancer. World J Clin Oncol. 2014;5(2):125-33. doi: 10.5306/wjco.v5.i2.125. PubMed PMID: 24829859; PubMed Central PMCID: PMCPMC4014784.
4. Nakamura S, Yagata H, Ohno S, Yamaguchi H, Iwata H, Tsunoda N, et al. Multi-center study evaluating circulating tumor cells as a surrogate for response to treatment and overall survival in metastatic breast cancer. Breast Cancer. 2010;17(3):199-204. doi: 10.1007/s12282-009-0139-3. PubMed PMID: 19649686.
5. Perou CM, Sorlie T, Eisen MB, van de Rijn M, Jeffrey SS, Rees CA, et al. Molecular portraits of human breast tumours. Nature. 2000;406(6797):747-52. doi: 10.1038/35021093. PubMed PMID: 10963602.
6. Masood S. Breast cancer subtypes: morphologic and biologic characterization. Womens Health (Lond). 2016;12(1):103-19. doi: 10.2217/whe.15.99. PubMed PMID: 26756229.
7. Vuong D, Simpson PT, Green B, Cummings MC, Lakhani SR. Molecular classification of breast cancer. Virchows Arch. 2014;465(1):1-14. doi: 10.1007/s00428-014-1593-7. PubMed PMID: 24878755.
8. Cancer Genome Atlas N. Comprehensive molecular portraits of human breast tumours. Nature. 2012;490(7418):61-70. doi: 10.1038/nature11412. PubMed PMID: 23000897; PubMed Central PMCID: PMCPMC3465532.
9. Goldhirsch A, Wood WC, Coates AS, Gelber RD, Thurlimann B, Senn HJ, et al. Strategies for subtypes--dealing with the diversity of breast cancer: highlights of the St. Gallen International Expert Consensus on the Primary Therapy of Early Breast Cancer 2011. Ann Oncol. 2011;22(8):1736-47. doi: 10.1093/annonc/mdr304. PubMed PMID: 21709140; PubMed Central PMCID: PMCPMC3144634.
10. Zielinska HA, Bahl A, Holly JM, Perks CM. Epithelial-to-mesenchymal transition in breast cancer: a role for insulin-like growth factor I and insulin-like growth factor-binding protein 3? Breast Cancer (Dove Med Press). 2015;7:9-19. doi: 10.2147/BCTT.S43932. PubMed PMID: 25632238; PubMed Central PMCID: PMCPMC4304531.
11. Siegel RL, Miller KD, Jemal A. Cancer statistics, 2016. CA Cancer J Clin. 2016;66(1):7-30. doi: 10.3322/caac.21332. PubMed PMID: 26742998.
12. Schwartz RS, Erban JK. Timing of Metastasis in Breast Cancer. N Engl J Med. 2017;376(25):2486-8. doi: 10.1056/NEJMcibr1701388. PubMed PMID: 28636861.
13. Lee RC, Feinbaum RL, Ambros V. The C. elegans heterochronic gene lin-4 encodes small RNAs with antisense complementarity to lin-14. Cell. 1993;75(5):843-54. PubMed PMID: 8252621.
14. Winter J, Jung S, Keller S, Gregory RI, Diederichs S. Many roads to maturity: microRNA biogenesis pathways and their regulation. Nat Cell Biol. 2009;11(3):228-34. doi: 10.1038/ncb0309-228. PubMed PMID: 19255566.
15. Macfarlane LA, Murphy PR. MicroRNA: Biogenesis, Function and Role in Cancer. Curr Genomics. 2010;11(7):537-61. doi: 10.2174/138920210793175895. PubMed PMID: 21532838; PubMed Central PMCID: PMCPMC3048316.
16. Ha M, Kim VN. Regulation of microRNA biogenesis. Nat Rev Mol Cell Biol. 2014;15(8):509-24. doi: 10.1038/nrm3838. PubMed PMID: 25027649.

17. Kozomara A, Griffiths-Jones S. miRBase: annotating high confidence microRNAs using deep sequencing data. Nucleic Acids Res. 2014;42(Database issue):D68-73. doi: 10.1093/nar/gkt1181. PubMed PMID: 24275495; PubMed Central PMCID: PMCPMC3965103.
18. Takahashi RU, Miyazaki H, Ochiya T. The Roles of MicroRNAs in Breast Cancer. Cancers (Basel). 2015;7(2):598-616. doi: 10.3390/cancers7020598. PubMed PMID: 25860815; PubMed Central PMCID: PMCPMC4491673.
19. Graveel CR, Calderone HM, Westerhuis JJ, Winn ME, Sempere LF. Critical analysis of the potential for microRNA biomarkers in breast cancer management. Breast Cancer (Dove Med Press). 2015;7:59-79. doi: 10.2147/BCTT.S43799. PubMed PMID: 25759599; PubMed Central PMCID: PMCPMC4346363.
20. Blenkiron C, Goldstein LD, Thorne NP, Spiteri I, Chin SF, Dunning MJ, et al. MicroRNA expression profiling of human breast cancer identifies new markers of tumor subtype. Genome Biol. 2007;8(10):R214. doi: 10.1186/gb-2007-8-10-r214. PubMed PMID: 17922911; PubMed Central PMCID: PMCPMC2246288.
21. de Rinaldis E, Gazinska P, Mera A, Modrusan Z, Fedorowicz GM, Burford B, et al. Integrated genomic analysis of triple-negative breast cancers reveals novel microRNAs associated with clinical and molecular phenotypes and sheds light on the pathways they control. BMC Genomics. 2013;14:643. doi: 10.1186/1471-2164-14-643. PubMed PMID: 24059244; PubMed Central PMCID: PMCPMC4008358.
22. Altuvia Y, Landgraf P, Lithwick G, Elefant N, Pfeffer S, Aravin A, et al. Clustering and conservation patterns of human microRNAs. Nucleic Acids Res. 2005;33(8):2697-706. doi: 10.1093/nar/gki567. PubMed PMID: 15891114; PubMed Central PMCID: PMCPMC1110742.
23. Frankel LB, Christoffersen NR, Jacobsen A, Lindow M, Krogh A, Lund AH. Programmed cell death 4 (PDCD4) is an important functional target of the microRNA miR-21 in breast cancer cells. J Biol Chem. 2008;283(2):1026-33. doi: 10.1074/jbc.M707224200. PubMed PMID: 17991735.
24. Huber MA, Azoitei N, Baumann B, Grunert S, Sommer A, Pehamberger H, et al. NF-kappaB is essential for epithelial-mesenchymal transition and metastasis in a model of breast cancer progression. J Clin Invest. 2004;114(4):569-81. doi: 10.1172/JCI21358. PubMed PMID: 15314694; PubMed Central PMCID: PMCPMC503772.
25. Korpal M, Lee ES, Hu G, Kang Y. The miR-200 family inhibits epithelial-mesenchymal transition and cancer cell migration by direct targeting of E-cadherin transcriptional repressors ZEB1 and ZEB2. J Biol Chem. 2008;283(22):14910-4. doi: 10.1074/jbc.C800074200. PubMed PMID: 18411277; PubMed Central PMCID: PMCPMC3258899.
26. Yadav P, Mirza M, Nandi K, Jain SK, Kaza RC, Khurana N, et al. Serum microRNA-21 expression as a prognostic and therapeutic biomarker for breast cancer patients. Tumour Biol. 2016;37(11):15275-82. doi: 10.1007/s13277-016-5361-y. PubMed PMID: 27696295.
27. Garzon R, Pichiorri F, Palumbo T, Iuliano R, Cimmino A, Aqeilan R, et al. MicroRNA fingerprints during human megakaryocytopoiesis. Proc Natl Acad Sci U S A. 2006;103(13):5078-83. doi: 10.1073/pnas.0600587103. PubMed PMID: 16549775; PubMed Central PMCID: PMCPMC1458797.
28. Wang J, Zhou Y, Fei X, Chen X, Yan J, Liu B, et al. ADAM9 functions as a promoter of gastric cancer growth which is negatively and post-transcriptionally regulated by miR-126. Oncol Rep. 2017;37(4):2033-40. doi: 10.3892/or.2017.5460. PubMed PMID: 28260063.
29. Han IB, Kim M, Lee SH, Kim JK, Kim SH, Chang JH, et al. Down-regulation of MicroRNA-126 in Glioblastoma and its Correlation with Patient Prognosis: A Pilot Study. Anticancer Res. 2016;36(12):6691-7. doi: 10.21873/anticanres.11280. PubMed PMID: 27920004.
30. Zhang Y, Yang P, Sun T, Li D, Xu X, Rui Y, et al. miR-126 and miR-126* repress recruitment of mesenchymal stem cells and inflammatory monocytes to inhibit breast cancer metastasis. Nat Cell Biol. 2013;15(3):284-94. doi: 10.1038/ncb2690. PubMed PMID: 23396050; PubMed Central PMCID: PMCPMC3672398.

31. Du C, Lv Z, Cao L, Ding C, Gyabaah OA, Xie H, et al. MiR-126-3p suppresses tumor metastasis and angiogenesis of hepatocellular carcinoma by targeting LRP6 and PIK3R2. J Transl Med. 2014;12:259. doi: 10.1186/s12967-014-0259-1. PubMed PMID: 25240815; PubMed Central PMCID: PMCPMC4189615.
32. Xiang LY, Ou HH, Liu XC, Chen ZJ, Li XH, Huang Y, et al. Loss of tumor suppressor miR-126 contributes to the development of hepatitis B virus-related hepatocellular carcinoma metastasis through the upregulation of ADAM9. Tumour Biol. 2017;39(6):1010428317709128. doi: 10.1177/1010428317709128. PubMed PMID: 28639884.
33. Xiong Y, Kotian S, Zeiger MA, Zhang L, Kebebew E. miR-126-3p Inhibits Thyroid Cancer Cell Growth and Metastasis, and Is Associated with Aggressive Thyroid Cancer. PLoS One. 2015;10(8):e0130496. doi: 10.1371/journal.pone.0130496. PubMed PMID: 26244545; PubMed Central PMCID: PMCPMC4526518.
34. Jiang L, He A, Zhang Q, Tao C. miR-126 inhibits cell growth, invasion, and migration of osteosarcoma cells by downregulating ADAM-9. Tumour Biol. 2014;35(12):12645-54. doi: 10.1007/s13277-014-2588-3. PubMed PMID: 25213697.
35. Hansen TF, Carlsen AL, Heegaard NH, Sorensen FB, Jakobsen A. Changes in circulating microRNA-126 during treatment with chemotherapy and bevacizumab predicts treatment response in patients with metastatic colorectal cancer. Br J Cancer. 2015;112(4):624-9. doi: 10.1038/bjc.2014.652. PubMed PMID: 25584492; PubMed Central PMCID: PMCPMC4333496.
36. Tavazoie SF, Alarcon C, Oskarsson T, Padua D, Wang Q, Bos PD, et al. Endogenous human microRNAs that suppress breast cancer metastasis. Nature. 2008;451(7175):147-52. doi: 10.1038/nature06487. PubMed PMID: 18185580; PubMed Central PMCID: PMCPMC2782491.
37. Dumeaux V, Borresen-Dale AL, Frantzen JO, Kumle M, Kristensen VN, Lund E. Gene expression analyses in breast cancer epidemiology: the Norwegian Women and Cancer postgenome cohort study. Breast cancer research. 2008;10(1):R13. Epub 2008/02/15. doi: 10.1186/bcr1859. PubMed PMID: 18271962; PubMed Central PMCID: PMCPmc2374969.
38. Coates AS, Winer EP, Goldhirsch A, Gelber RD, Gnant M, Piccart-Gebhart M, et al. Tailoring therapies--improving the management of early breast cancer: St Gallen International Expert Consensus on the Primary Therapy of Early Breast Cancer 2015. Ann Oncol. 2015;26(8):1533-46. Epub 2015/05/06. doi: 10.1093/annonc/mdv221. PubMed PMID: 25939896; PubMed Central PMCID: PMCPmc4511219.
39. Vasconcelos I, Hussainzada A, Berger S, Fietze E, Linke J, Siedentopf F, et al. The St. Gallen surrogate classification for breast cancer subtypes successfully predicts tumor presenting features, nodal involvement, recurrence patterns and disease free survival. Breast. 2016;29:181-5. Epub 2016/08/22. doi: 10.1016/j.breast.2016.07.016. PubMed PMID: 27544822.
40. Bremnes RM, Veve R, Gabrielson E, Hirsch FR, Baron A, Bemis L, et al. High-Throughput Tissue Microarray Analysis Used to Evaluate Biology and Prognostic Significance of the E-Cadherin Pathway in Non–Small-Cell Lung Cancer. Journal of Clinical Oncology. 2002;20(10):2417-28. doi: doi:10.1200/JCO.2002.08.159. PubMed PMID: 12011119.
41. Johannessen C, Moi L, Kiselev Y, Pedersen MI, Dalen SM, Braaten T, et al. Expression and function of the miR-143/145 cluster in vitro and in vivo in human breast cancer. PLoS One. 2017;12(10):e0186658. doi: 10.1371/journal.pone.0186658. PubMed PMID: 29073169; PubMed Central PMCID: PMCPMC5657998.
42. Tahiri A, Leivonen SK, Luders T, Steinfeld I, Ragle Aure M, Geisler J, et al. Deregulation of cancer-related miRNAs is a common event in both benign and malignant human breast tumors. Carcinogenesis. 2014;35(1):76-85. doi: 10.1093/carcin/bgt333. PubMed PMID: 24104550.
43. Sezer Zhmurov C, Timirci-Kahraman O, Amadou FZ, Fazliogullari O, Basaran C, Catal T, et al. Expression of Egfl7 and miRNA-126-5p in Symptomatic Carotid Artery Disease. Genet Test Mol Biomarkers. 2016;20(3):125-9. doi: 10.1089/gtmb.2015.0252. PubMed PMID: 26799121.

44. Luo P, Fei J, Zhou J, Zhang W. microRNA-126 suppresses PAK4 expression in ovarian cancer SKOV3 cells. Oncology letters. 2015;9(5):2225-9. doi: 10.3892/ol.2015.3012. PubMed PMID: 26137045; PubMed Central PMCID: PMCPMC4467333.
45. Yang Z, Wang R, Zhang T, Dong X. MicroRNA-126 regulates migration and invasion of gastric cancer by targeting CADM1. Int J Clin Exp Pathol. 2015;8(8):8869-80. PubMed PMID: 26464628; PubMed Central PMCID: PMCPMC4583860.
46. Zhao C, Li Y, Zhang M, Yang Y, Chang L. miR-126 inhibits cell proliferation and induces cell apoptosis of hepatocellular carcinoma cells partially by targeting Sox2. Hum Cell. 2015;28(2):91-9. doi: 10.1007/s13577-014-0105-z. PubMed PMID: 25585946.
47. Ren G, Kang Y. A one-two punch of miR-126/126* against metastasis. Nat Cell Biol. 2013;15(3):231-3. doi: 10.1038/ncb2703. PubMed PMID: 23449143.
48. Shibayama Y, Kondo T, Ohya H, Fujisawa S, Teshima T, Iseki K. Upregulation of microRNA-126-5p is associated with drug resistance to cytarabine and poor prognosis in AML patients. Oncol Rep. 2015;33(5):2176-82. doi: 10.3892/or.2015.3839. PubMed PMID: 25759982; PubMed Central PMCID: PMCPMC4391586.
49. Schober A, Nazari-Jahantigh M, Wei Y, Bidzhekov K, Gremse F, Grommes J, et al. MicroRNA-126-5p promotes endothelial proliferation and limits atherosclerosis by suppressing Dlk1. Nat Med. 2014;20(4):368-76. Epub 2014/03/04. doi: 10.1038/nm.3487. PubMed PMID: 24584117; PubMed Central PMCID: PMCPMC4398028.
50. Gaelle V, Loic P, Baraa N, Gaelle B, Carlos RJ, Sylvain C, et al. miR-126-5p promotes retinal endothelial cell survival through SetD5 regulatio in neurons. Development. 2017. doi: 10.1242/dev.156232. PubMed PMID: 29180574.
51. Tao SC, Guo SC, Li M, Ke QF, Guo YP, Zhang CQ. Chitosan Wound Dressings Incorporating Exosomes Derived from MicroRNA-126-Overexpressing Synovium Mesenchymal Stem Cells Provide Sustained Release of Exosomes and Heal Full-Thickness Skin Defects in a Diabetic Rat Model. Stem Cells Transl Med. 2017;6(3):736-47. doi: 10.5966/sctm.2016-0275. PubMed PMID: 28297576; PubMed Central PMCID: PMCPMC5442792.
52. Nueda ML, Naranjo AI, Baladron V, Laborda J. Different expression levels of DLK1 inversely modulate the oncogenic potential of human MDA-MB-231 breast cancer cells through inhibition of NOTCH1 signaling. FASEB journal : official publication of the Federation of American Societies for Experimental Biology. 2017;31(8):3484-96. Epub 2017/05/04. doi: 10.1096/fj.201601341RRR. PubMed PMID: 28461338.
53. Shibayama Y, Kondo T, Ohya H, Fujisawa S-I, Teshima T, Iseki KEN. Upregulation of microRNA-126-5p is associated with drug resistance to cytarabine and poor prognosis in AML patients. Oncology reports. 2015;33(5):2176-82. doi: 10.3892/or.2015.3839. PubMed PMID: PMC4391586.
54. Wolf I, Levanon-Cohen S, Bose S, Ligumsky H, Sredni B, Kanety H, et al. Klotho: a tumor suppressor and a modulator of the IGF-1 and FGF pathways in human breast cancer. Oncogene. 2008;27(56):7094-105. Epub 2008/09/03. doi: 10.1038/onc.2008.292. PubMed PMID: 18762812.
55. Griffiths-Jones S, Hui JHL, Marco A, Ronshaugen M. MicroRNA evolution by arm switching. EMBO Reports. 2011;12(2):172-7. doi: 10.1038/embor.2010.191. PubMed PMID: PMC3049427.
56. Tsai K-W, Leung C-M, Lo Y-H, Chen T-W, Chan W-C, Yu S-Y, et al. Arm Selection Preference of MicroRNA-193a Varies in Breast Cancer. Scientific Reports. 2016;6:28176. doi: 10.1038/srep28176. PubMed PMID: PMC4910092.
57. Png KJ, Halberg N, Yoshida M, Tavazoie SF. A microRNA regulon that mediates endothelial recruitment and metastasis by cancer cells. Nature. 2011;481(7380):190-4. Epub 2011/12/16. doi: 10.1038/nature10661. PubMed PMID: 22170610.
58. Bussard KM, Mutkus L, Stumpf K, Gomez-Manzano C, Marini FC. Tumor-associated stromal cells as key contributors to the tumor microenvironment. Breast cancer research : BCR. 2016;18(1):84. Epub

2016/08/16. doi: 10.1186/s13058-016-0740-2. PubMed PMID: 27515302; PubMed Central PMCID: PMCPmc4982339.
59. Valadi H, Ekstrom K, Bossios A, Sjostrand M, Lee JJ, Lotvall JO. Exosome-mediated transfer of mRNAs and microRNAs is a novel mechanism of genetic exchange between cells. Nat Cell Biol. 2007;9(6):654-9. doi: 10.1038/ncb1596. PubMed PMID: 17486113.
60. Kogure T, Lin WL, Yan IK, Braconi C, Patel T. Intercellular nanovesicle-mediated microRNA transfer: a mechanism of environmental modulation of hepatocellular cancer cell growth. Hepatology. 2011;54(4):1237-48. doi: 10.1002/hep.24504. PubMed PMID: 21721029; PubMed Central PMCID: PMCPMC3310362.
61. Chiba M, Kimura M, Asari S. Exosomes secreted from human colorectal cancer cell lines contain mRNAs, microRNAs and natural antisense RNAs, that can transfer into the human hepatoma HepG2 and lung cancer A549 cell lines. Oncol Rep. 2012;28(5):1551-8. doi: 10.3892/or.2012.1967. PubMed PMID: 22895844; PubMed Central PMCID: PMCPMC3583404.
62. Shah SH, Miller P, Garcia-Contreras M, Ao Z, Machlin L, Issa E, et al. Hierarchical paracrine interaction of breast cancer associated fibroblasts with cancer cells via hMAPK-microRNAs to drive ER-negative breast cancer phenotype. Cancer Biol Ther. 2015;16(11):1671-81. Epub 2015/07/18. doi: 10.1080/15384047.2015.1071742. PubMed PMID: 26186233; PubMed Central PMCID: PMCPMC4846097.

Figures

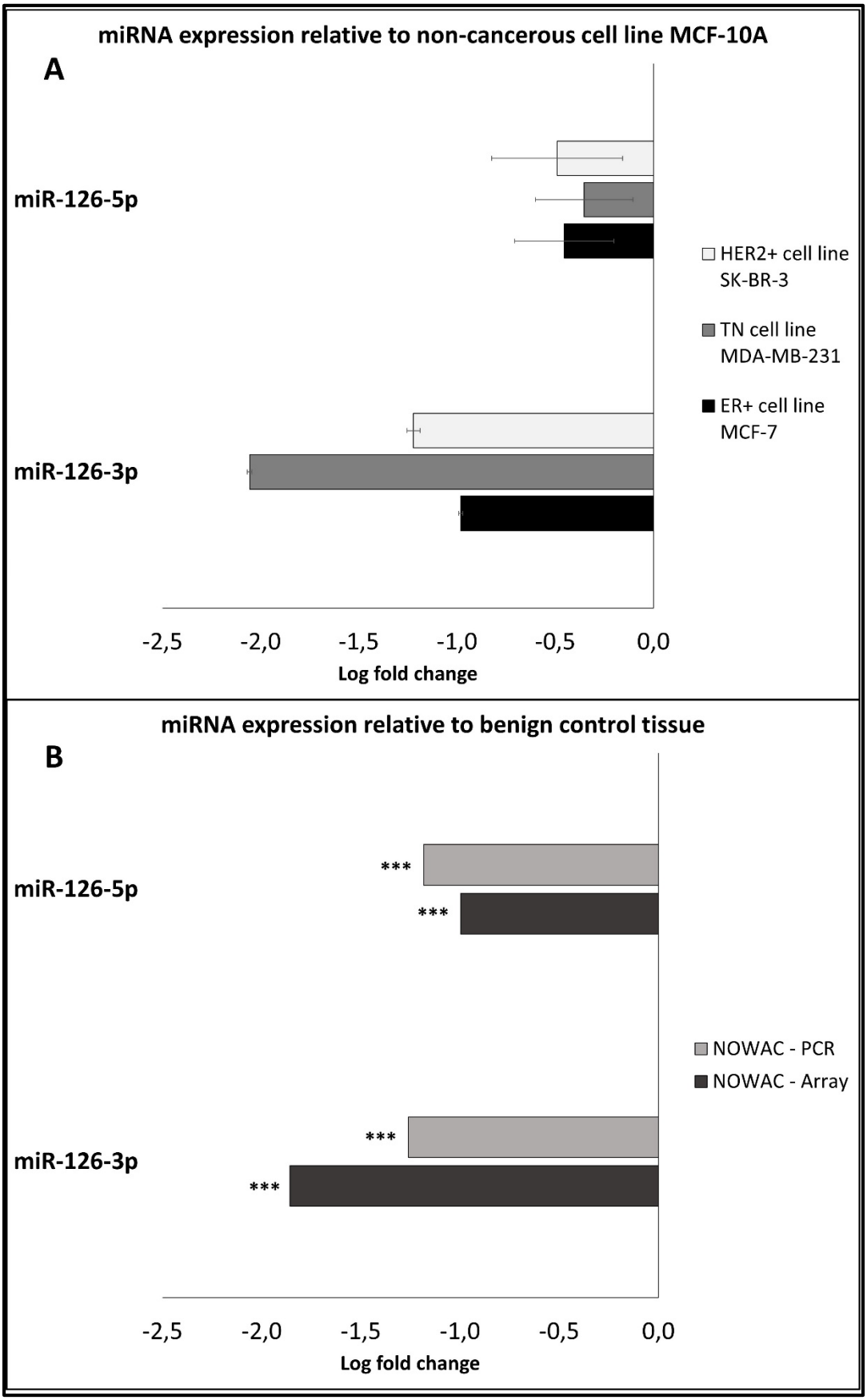

Fig. 1 – Endogenous expression. Endogenous miR-126 expression in three BC cell lines relative to the non-cancerous breast cell line MCF-10A (A), and the endogenous expression in BC tumors compared to benign breast tissue (B). Cell line data is displayed as mean log fold change ±SE from a representative biological replicate. The annotation *** signifies P<0.001 using the Mann–Whitney *U* test for independent samples.

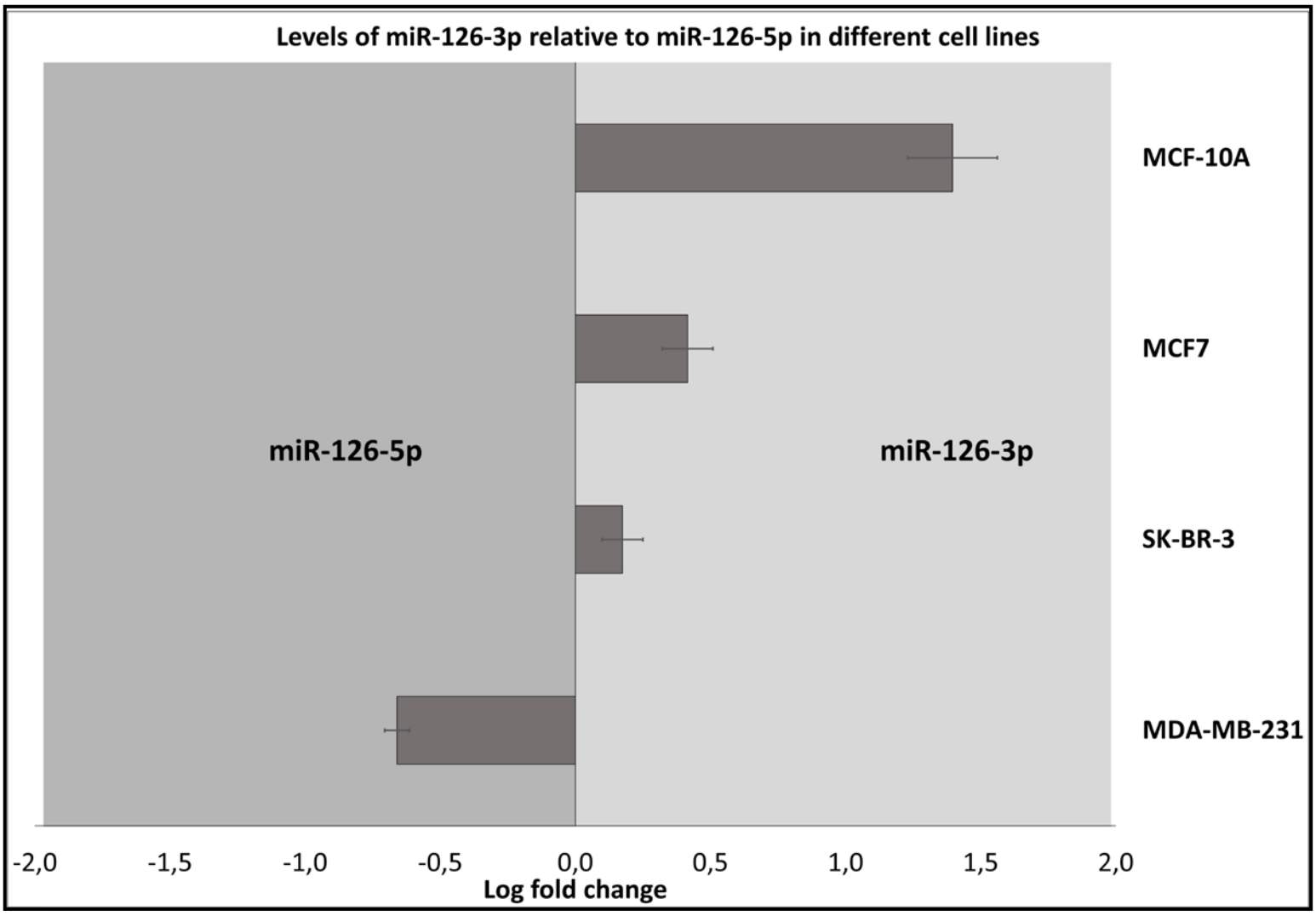

Fig. 2 – Expression pattern. The relative expression pattern between miR-126-3p and miR-126-5p in different breast cell lines. Based on RT-qPCR data, the relationship between miR-126-3p and miR-126-5p was studied in the non-cancerous breast cell line MCF-10A, the ER+ BC cell line MCF7, the HER2+ BC cell line SK-BR-3 and the TN BC cell line MDA-MB-231. Data are displayed as mean log fold change ±SE from a representative biological replicate.

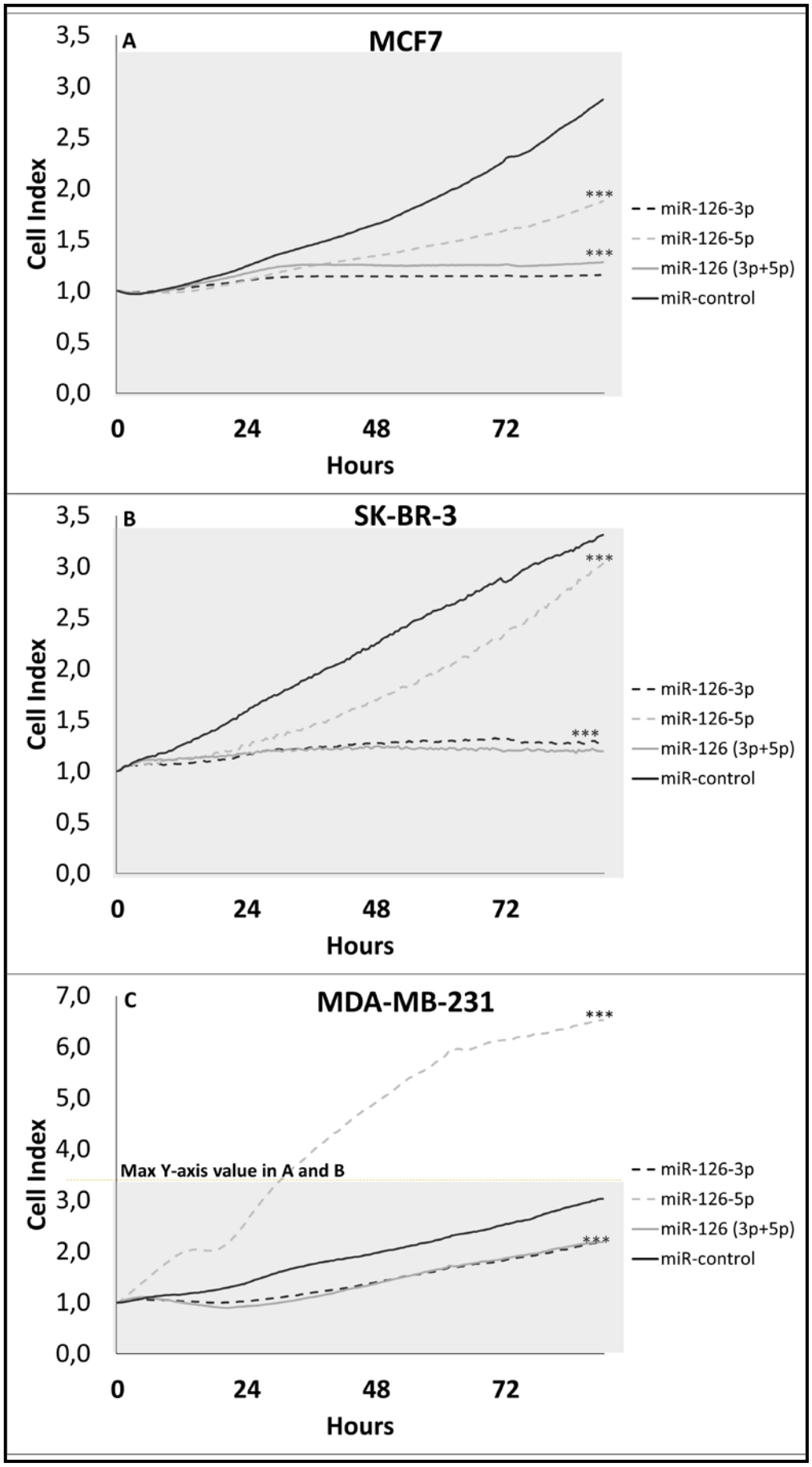

Fig. 3 - Proliferation. Experimental study on BC cell lines transfected with miR-126 performed in real-time using the xCelligence system. Proliferation in different BC cell lines after transfection with either miR-126-3p mimic, miR-126-p mimic or mimics 3p+5p in combination and equal concentration. Proliferation was assessed for the ER+ BC cell line MCF7 (A), the HER2+ BC cell line SK-BR-3 (B) and the TN BC cell line MDA-MB-231. Results are representative for all biological replicate, and each experiment includes four technical replicates. The annotation *** signifies P<0.001 with one-way ANOVA and the Benjamini & Hochberg correction comparing different transfections to controls.

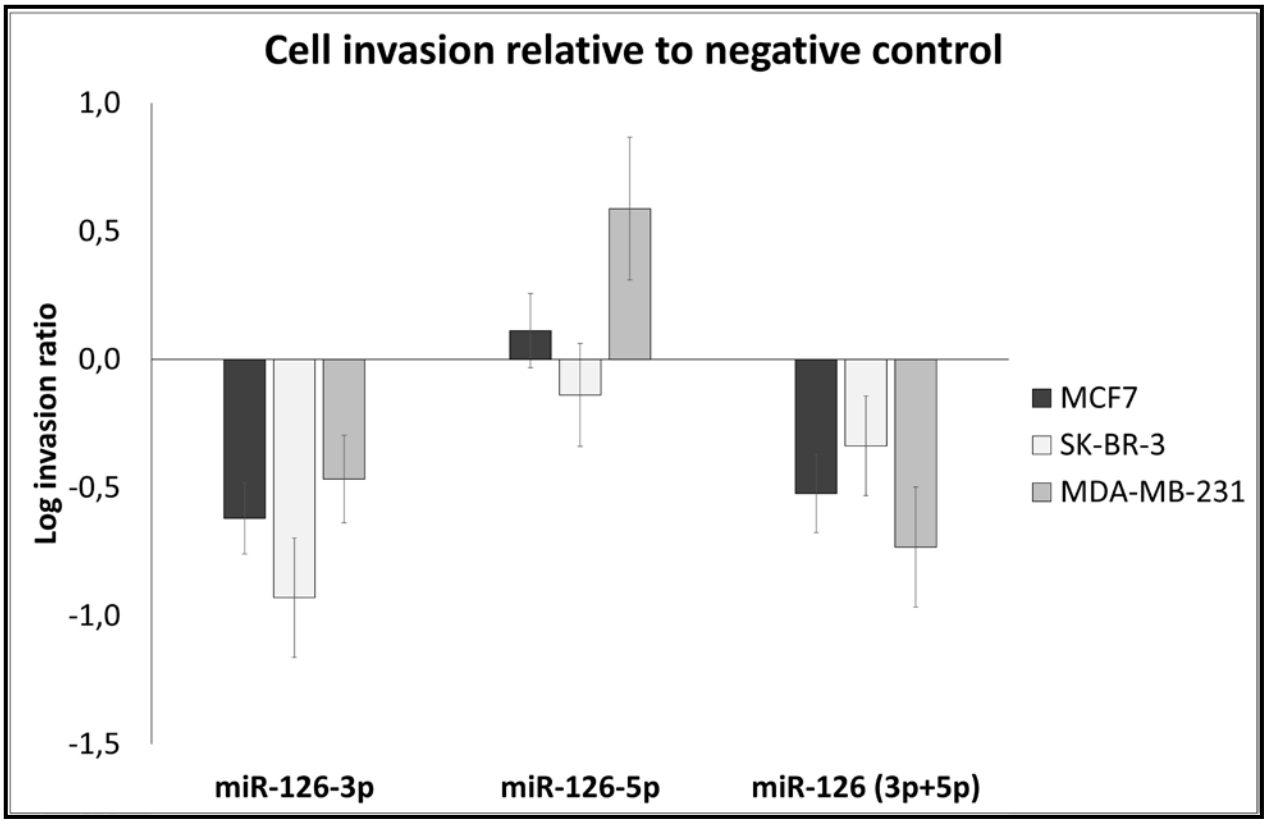

Fig. 4 – Invasion. Experimental study on invasion to assess the invasion potential in BC cell lines transfected with miR-126 performed using a Boyden chamber assay coated with a basement membrane matrix. BC cell lines transfected with either miR-126-3p, miR-126-5p or miR-126-3p + miR-126-5p in equal concentrations, were seeded in the upper wells of a modified Boyden chamber assay. Cells were allowed to invade, and migrate through, the basement membrane towards the bottom chamber containing bovine serum as a chemoattractant. Results are displayed as mean log fold change ±SD of miR-126 transfected cells relative to miR-control transfected cells. Data presented are from a representative biological experiment, which include four technical replicates for each cell line.

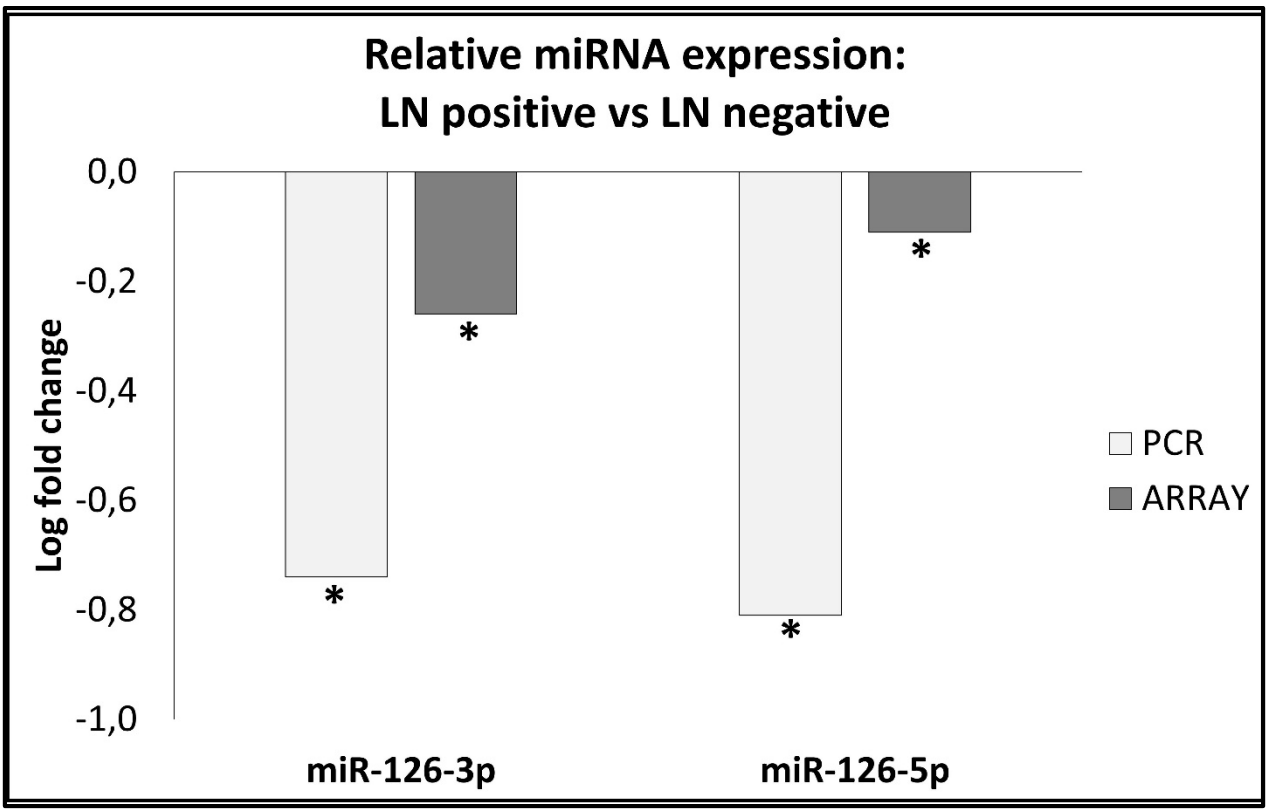

Fig. 5 – Nodal involvement. Differential expression of miR-126-3p and miR-126-5p in cancer patients with nodal involvement compared to patients with no nodal involvement. Results are displayed for both the miRNA microarray and the qPCR validation. Data are displayed as log fold change of nodal involvement vs no nodal involvement, and the annotation * signifies $P<0.05$.

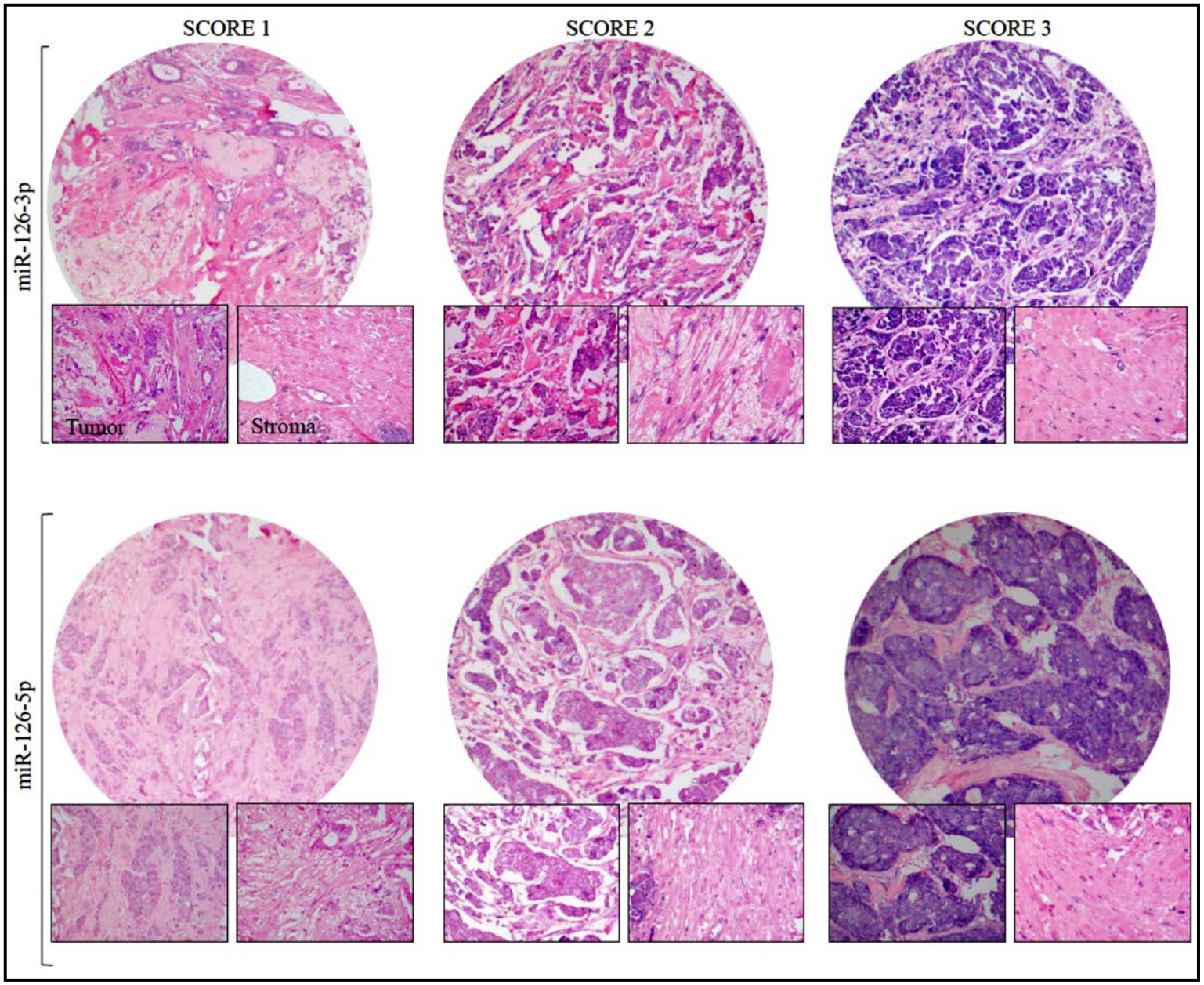

Fig. 6 – Intensities of ISH staining. The *in situ* hybridization staining intensities for miR-126-3p and miR-126-5p in TMA samples. TMA scores were analyzed in both tumor and stroma

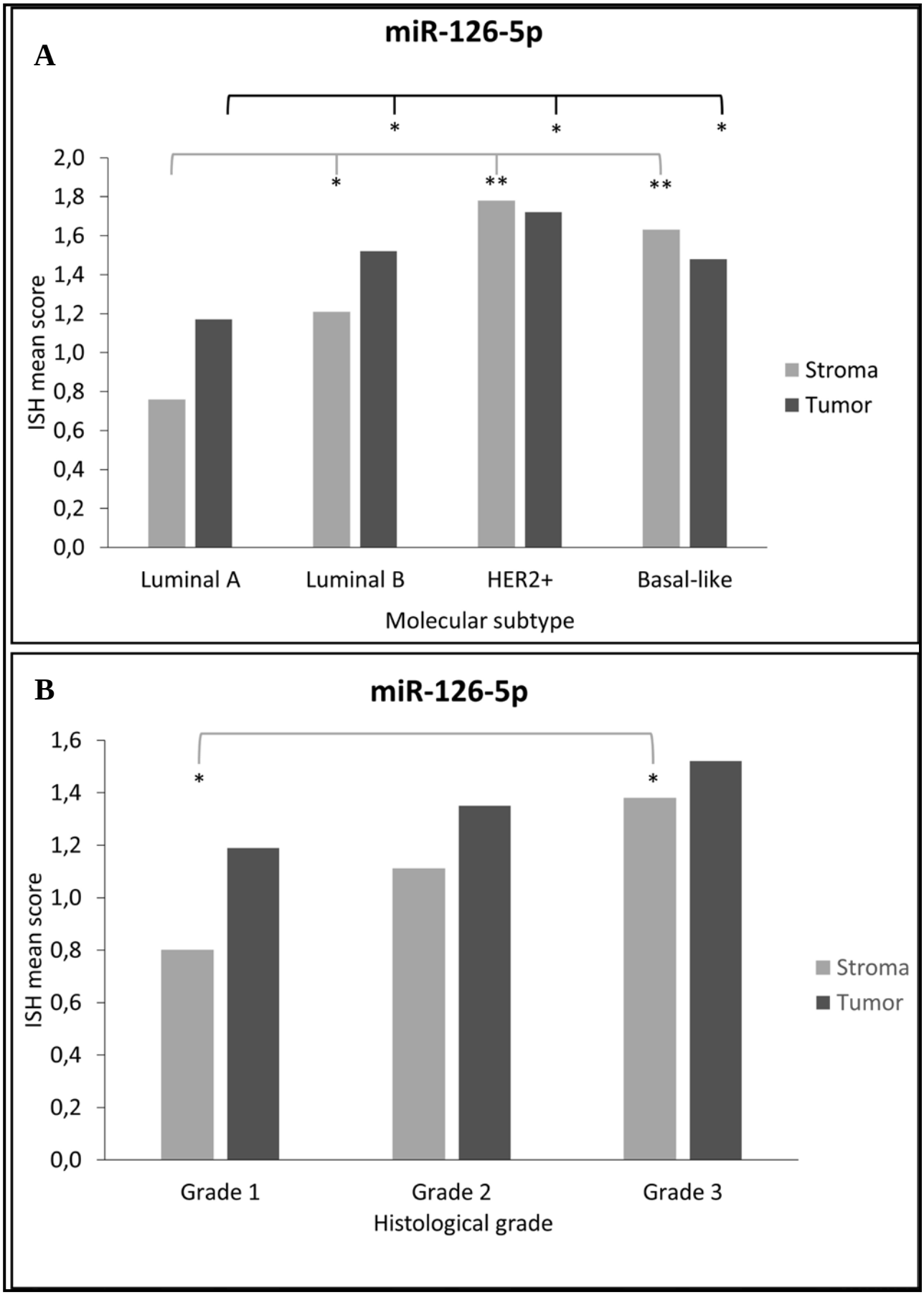

Fig. 7 – TMA subgroup analysis. Differential expression of miR-126-5p in TMA samples for tumor and stroma. Mean value of TMA-scoring stratified into molecular subtype (A) and histological grade (B). The annotation * and ** signifies $P<0.05$ and $P<0.01$, respectively.

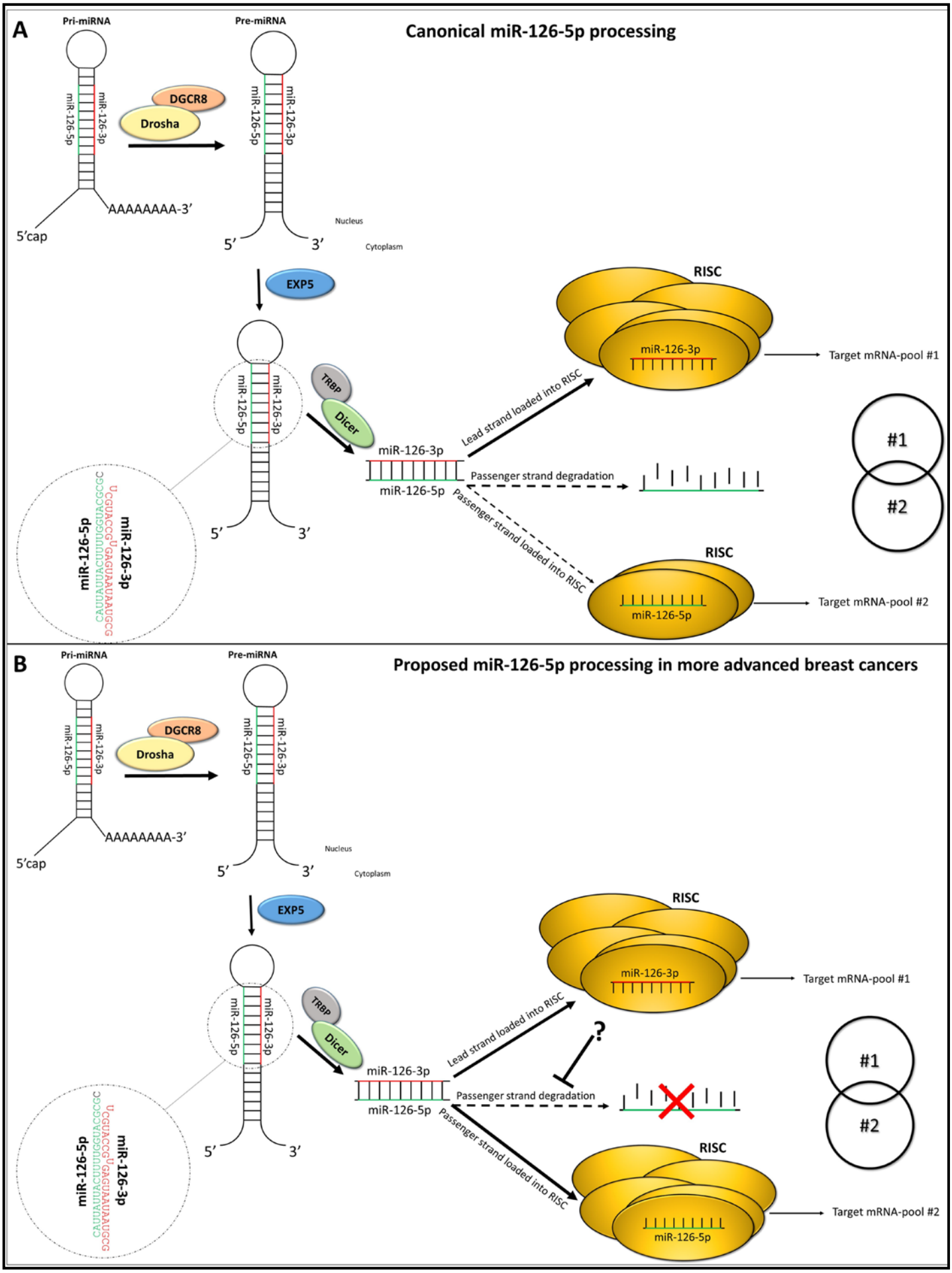

Fig. 8 – miR-126-5p processing in more advanced BC. Canonical processing of miR-126-5p (A), and our proposed miR-126-5p processing in more advanced cancer (B).